

Full path Monte Carlo simulation of fluorescence in non-voxelized complex heterogeneous mouse model

Jean-Francois Delorme*^a, Guobin Ma^a, Frederic Lesage^b,
Frederic Leblond^a, Anader Benyamin-Seyar^a

^aAdvanced Research Technologies, 2300 Alfred Nobel, Saint-Laurent, Qc, Canada H4S 2A4

^bEcole Polytechnique de Montreal, Electrical Engineering Department

ABSTRACT

In this article we propose an approach to improve the Monte Carlo simulation accuracy by implementing a full photon path integration simulation in a non-voxelized complex three-dimensional heterogeneous model. Mouse body shape, organs optical heterogeneities and fluorophore distribution are simulated by using boundary surface elements and basic analytical shapes. In addition, external and internal surface roughness and refractive index mismatch for complex angular objects are also considered and results are briefly compared with time sampled space voxelized Monte Carlo code, in order to illustrate the impact of these improvements on the simulation results.

Keywords: Monte Carlo Simulation, Fluorescence, Heterogeneous model

1. INTRODUCTION

In-vivo estimation of the localization and concentration of fluorescence-tagged agents in pre-clinical pharmacological studies and cancer research work is of tremendous importance. To develop and improve on the performance of quantitative fluorescence tomographic systems, accurate simulations of light propagation in complex heterogeneous models are needed. The proposed approach in this work is to improve upon current Monte Carlo simulation accuracy by implementing a full photon path integration simulation in a non-voxelized complex three-dimensional heterogeneous model. Mouse shape, organs optical heterogeneities and fluorophore distribution are simulated using boundary surface elements and basic analytical shapes. We propose a simple model to simulate the scattering effect of rough surface and to model fluorescence processes for complex angular objects. Results are briefly compared with well-known time sampling, space voxelized Monte Carlo code, in order to illustrate the impact of these improvements on the simulation results.

Monte Carlo simulations of diffusion processes have been used since the creation of computers [1][2][3]. Its application to photon diffusion inside biological tissues has been developed more than 20 years ago [4][5]. Computer processing power increased tremendously since then and complexity of fine calculations, which were unthinkable in the past without large-scale computer platforms is now possible with high performance personal computers.

We have investigated different Monte Carlo simulation tools for which the source code is freely available: MC321[7], MCML[8] and tMCimg[6]. In this article we describe improvements on those Monte Carlo simulations, which lead to more accurate results and allow simulations of photon diffusion and fluorescence processes inside a complex heterogeneous medium like the entire mouse anatomy.

*jfdelorm@art.ca; phone: (514) 832-0777 ext:315 fax: (514) 832-0778; www.art.ca

2. IDENTIFICATION OF SOME ISSUES WITH THE CURRENT MONTE CARLO SIMULATION IMPLEMENTATION

This work started when using publicly available implementations of Monte Carlo (MC) simulators. When working in particular geometries, as we will show in this article, some issues were found that are not handled by conventional Monte Carlo codes. A first issue is linked to the technique of time, distance and space sampling and associated discretization, which causes artifacts when not carefully adjusted. A second issue is linked to the geometric modeling of heterogeneous complex medium, which does not allow to adequately manage reflection and refraction at curved surfaces. Problems related to the modeling of rough surfaces were identified, which are usually neglected in MC simulations. Finally, fluorescence simulations can be improved to better represent reality and to achieve higher accuracy and precision of results.

2.1 Time-distance and space sampling

The first issues in conventional Monte Carlo are linked to the time or distance sampling approach used in the simulation. In codes like MC321[7], MCML[8] or tMCimg[6], photons paths are sampled at specific times (equivalent to specific distances of the photons paths). Photons packets are then scored in absorption or fluence voxelized result volume matrices. The time or distance sampling steps used for scoring and associated volume discretization is critical in some situation. Let us study the example, in a medium with low scattering and near the source, if the sampling step is too large (Fig.1a), photons could step over voxels without scoring any fluence, causing reduced and inaccurate values for those voxels. Even when the sampling step is smaller than the spatial discretization size (Fig.1b), artifacts occur because double or multiple scoring appears on some voxels, generating a repetitive pattern artifact. Reducing these discretization artifacts near the source or in low scattering medium necessitates a higher sampling rate (Fig. 1c), but at the expense of a reduced performance. Changes in the medium properties can also lead to variations in the effective sampling rate in the presence of large changes of refractive index. This could change the noise variance, which would then be interpreted as artifacts.

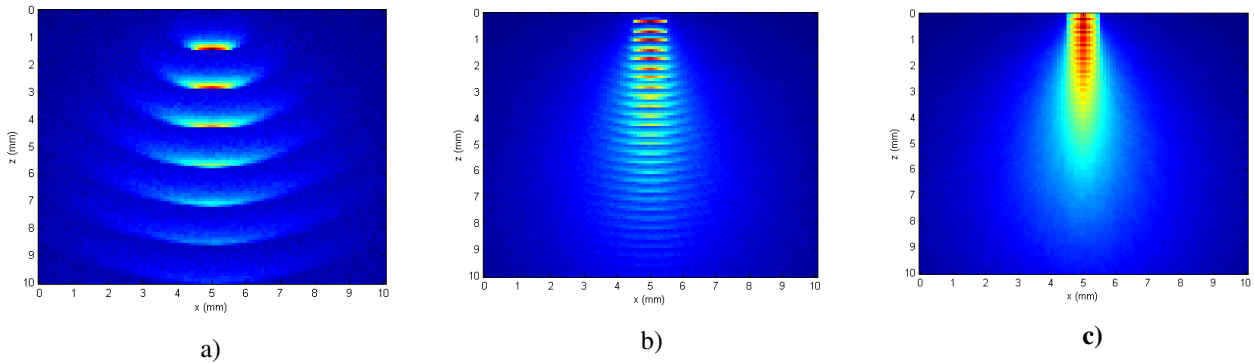


Fig. 1. Time-distance sampling artifacts for different sampling steps

Furthermore, for highly absorbing medium, when the sampling rate is in the same order of magnitude as the discretization size, if the photon path sampling position is at the beginning of the discretization, the logged fluence will be overestimated. If it is at the end of a discretization, it will be underestimated.

When scattering is high, or at large distances from the source, sampling and discretization effects are compensated by diffusion. The issues mentioned above have been neglected in the literature [6] without any impact assessment. Since previous work was mostly interested in large distance simulations, such as human head studies where photons become highly scattered in the region of interest. But this is not the case when performing simulations at shallow depths when working with small animals such as mice.

2.2 Angular surface geometric modeling

In current Monte Carlo implementations, heterogeneous mediums are modeled by voxelized geometries. This implies that reflections at angular surfaces (angle different from 0° or 90°) are inadequately managed. Increasing model resolution has no effect, since photons paths will always cross a horizontal or a vertical voxel interface.

2.3 Surface Roughness effect

When photons cross a rough surface between two media with different refractive indexes, at the macroscopic level, scattering occurs, even if the two materials are transparent. This is due to the fact that the microscopic distribution of surface angles is causing multiple refractions and/or reflections at the interface. Neglecting this rough surface effect could induce significant errors in certain cases[9]. Rough surfaces cause an increase in the photon scattering, which cannot be modeled by an increase in the scattering coefficient since it is a one time scattering event, having no effect once photons are inside the medium.

2.4 Fluorescence modeling

One of current approaches in Monte Carlo fluorescence tomography is to use the Born approximation and build a sensitivity matrix by Monte Carlo simulations. Here a source is positioned at both the illumination and detection points and a reversibility principle is used to build the sensitivity matrix [10]. This scheme reduces the processing time by orders of magnitude. In a time domain analysis, photons time arrivals can be calculated by convolving the exponential decay of the specific fluorescent compound with the photons time arrivals distribution of the two simulations, taking into account the fluorophore quantum efficiency and the extinction coefficient.

Unfortunately this approach has its limitations. To apply the principle of reversibility, photons propagating from point B to point A are equivalent to photons propagated from point A to point B, if the angular distributions are equivalent respectively. This is true for an isotropic source and an idealized detector. If the detection is far from the source and photons reach a diffusion regime that could be considered isotropic, then the detection angular distribution can be estimated. For shallow depth reflections and for small volume simulations, in low scattering medium, this angular distribution is not known and using the current approach can lead to large quantification errors. A simple example is when a photon beam enters a low scattering and low absorbing medium. A fluorescent volume under the beam could receive a large percentage of the injected photons. But we cannot say that the same percentage of the fluorescent reemitted photons will reach the detector, since they might be only a very small fraction of them will reach it depending on the detector geometry.

Another important fluorescence phenomenon is photon reabsorption and reemission causing an increase of the effective lifetime, meaning a longer exponential decay of detected photon arrival time distribution. In certain cases, e.g. for high concentration fluorescent compound, this phenomenon may impact the results considerably.

3. PROPOSED MC SIMULATION IMPROVEMENTS

3.1 Non sampling fluence affectation

There are two definitions for the photon fluence. The first is: the integral of all photons crossing a small infinitesimal spherical transparent volume, divided by the area of its cross section [11].

$$\Phi = \frac{dN}{dA} \quad (1)$$

Where N is the number of photons crossing the region, and A is the region cross section

The second definition, which is more appropriate in our case, is the sum of photon paths inside the region, divided by the region volume [12]:

$$\Phi = \frac{\sum dL}{dV} \quad (2)$$

Where L is the photon path inside the region and V is the region volume

Our proposed approach is based on removing the spatial sampling of the photons paths and use of the second definition in the calculation of fluence. The fluence calculation scheme (Fig. 2) consists in the following: for each photon paths between scattering events, identify the intersection points with the fluence volume x-y-z discretization planes. Then between each intersection point, the fluence is calculated by integrating the photon packet weight.

$$\Phi_{ab} = \left(\int_a^b I_0 \cdot e^{-\mu_a l} dl \right) / dV \quad (3)$$

The mid point between the two intersections is calculated and the calculated fluence is affected to the voxel containing the mid point.

The advantage of this approach is that fluence quantification is preserved. For a specific photon path distance, the integration of the affected fluence is independent from the discretization. This is different from the sampling approach, where the integration of the affected fluence is dependant on the space discretization and the photon path time or distance sampling.

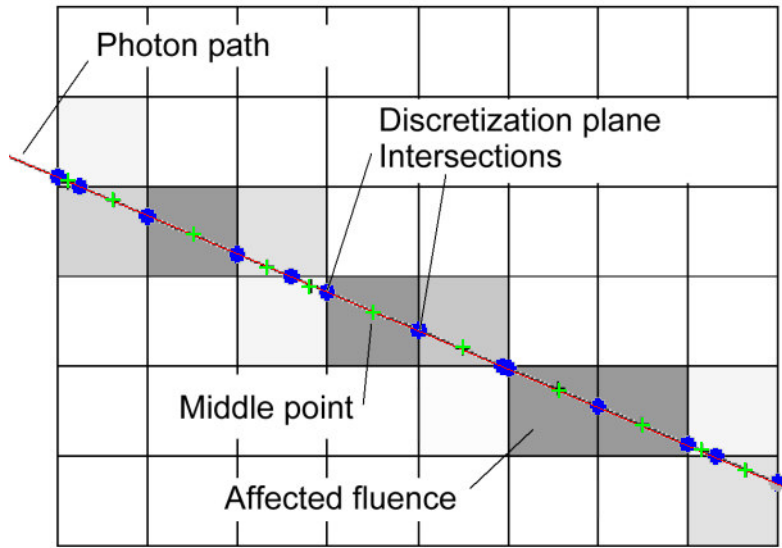


Fig. 2. Fluence affectation

3.2 Non voxelized geometry

To be able to manage reflection and refraction at angular surfaces correctly, an ideal solution is to use an analytical representation of those surfaces. This can be done for simple geometrical objects, but for complex objects such as an entire mouse anatomy, polygonal meshes are a much more practical solution. The use of polygonal mesh has the advantages that very fast algorithms [13][14] do exist to test photons paths intersections with the volume surface model in the simulations.

To simulate an example of a complex medium, we have generated a mesh of the Moby Mouse [15] using the control points of the NURBS surface from the original data (Fig. 3).

The challenge of MC simulation with this kind of geometry is that at every photon step, intersection tests should be performed with the modeled surfaces. Testing all polygonal elements would incur an unacceptable processing time. Fortunately, different optimization schemes exist to reduce processing time to a minimum, by reducing the number of those intersection tests. The implemented scheme here is to use a hierarchical elimination strategy, using global bounding box tests for organs followed by polygonal elements bounding box test. Pre-calculating surface normals and surface parameters was also implemented to reduce processing time.

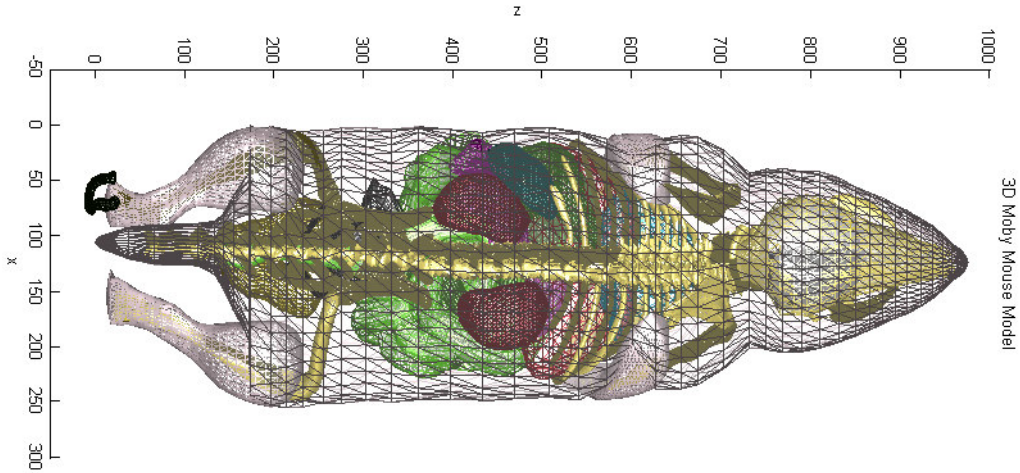


Fig. 3. NURBS control points meshed Moby mouse[15]

To show the advantages of using a non-voxelized geometry, we simulated a free beam hitting the side of a cylindrical scattering medium (with $\mu_s=10 \text{ mm}^{-1}$, $\mu_a= 0.03 \text{ mm}^{-1}$, $g=0.90$ and $n=1.4$). The first simulation (Fig. 4) was performed using tMCimg and the second (Fig. 5) with our enhanced MC simulator managing angular interfaces. In (Fig.4) we observe that no refraction occurs at the angular interface as for the second simulation (Fig. 5) we can see the fluence of the reflected beam in air and the change of direction of the refracted beam inside the scattering medium.

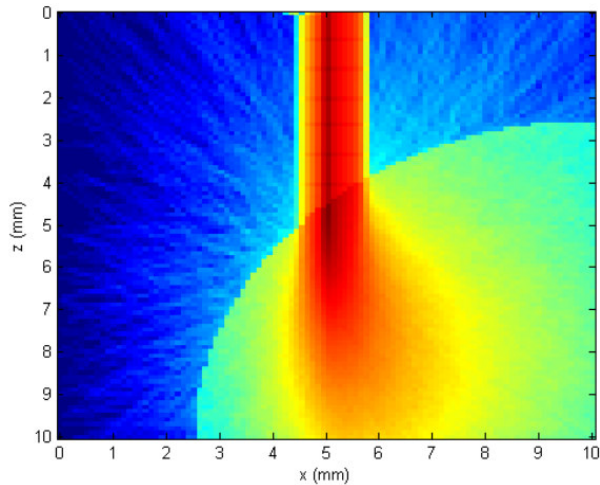


Fig. 4. TMCimg: fluence projection of a free beam hitting the side of a cylindrical scattering medium $n_1=1.0$, $n_2=1.4$ (voxelized geometry)

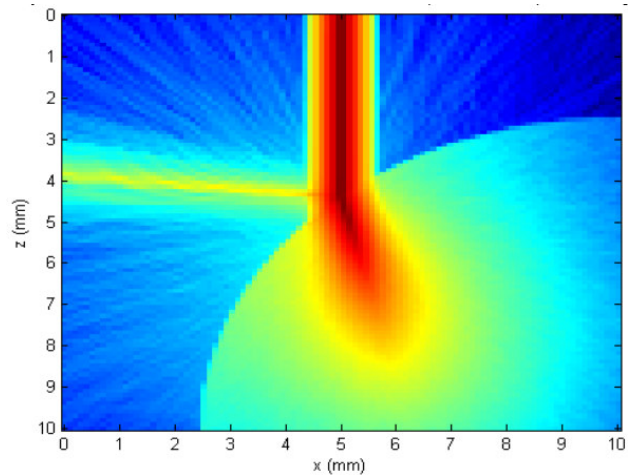


Fig. 5. Proposed Approach: fluence projection of a free beam hitting the side of a cylindrical scattering medium $n_1=1.0$, $n_2=1.4$ (angular surface geometry)

Below (Fig. 6) is an example of a simulation, using a non-voxelized entire mouse model [15] in the Monte Carlo simulation.

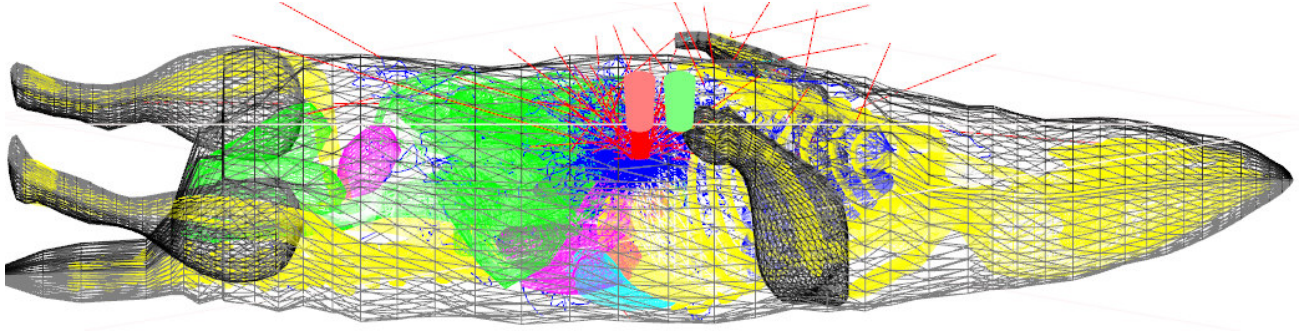


Fig. 6. MC Simulation using non-voxelized entire mouse model

In this model, each organ has been assigned its own optical properties and a specific fluorescence concentration. The photon path simulation does not use any voxel discretization, but affected fluence is done in voxelized geometry, in order to be able to visualize the results and use them in tomographic reconstruction algorithms for example.

3.3 Rough surface modeling

The challenge of the rough surface modeling, is to define a BSDF (Bi-directional Scattering Distribution Function) describing how the incident photons are reflected and/or refracted at the interface, excluding the diffusion processes, just modeling the roughness effect of the surface. The BSDF is the sum of the BRDF (Bi-directional Reflection Distribution Function), which describes the reflection part and the BTDF (Bi-directional Transmission Distribution Function) which describes the transmitted part. These functions model the angular distribution of reflected and refracted radiance as a function of incident radiance.

To model the surface roughness effect, different approaches were studied.

Physical or semi-physical based approaches [16][17] are very attractive, but no method can predict the surface BSDF without experimental measurements. Taking into account that even for complex BSDF models, parameters need to be fitted using experimental data, we decided to use a simple multi-component modeling approach.

In our proposed approach, a rough surface effect is modeled with three components (Fig. 7): an isotropic component, usually very small, a lambertian component and a specular lobe component. The total BSDF is defined by six parameters. The first three are the percentages of the isotropic, lambertian and specular lobe, one of these parameters being redundant since the sum of the three parameters equals 1.0. One parameter σ_θ represents the spread of the specular lobe. The last two parameters, one for the isotropic component $F_{iso/spec}$ and another one for the lambertian component $F_{lamb/spec}$, representing the dependence of the reflection and refraction parts on the Fresnel term. The Monte Carlo threshold to decide if photon is reflected or refracted is then calculated using:

$$Th_{R_{iso}} = F_{iso/spec} \cdot R + \frac{(1 - F_{iso/spec})}{2} \quad \text{and} \quad Th_{R_{lamb}} = F_{lamb/spec} \cdot R + \frac{(1 - F_{lamb/spec})}{2} \quad (3)$$

This mean that if the parameters are equal to zero then:

$$\frac{\int BTDF_i}{\int BRDF_i} = 1 \tag{4}$$

If the parameters equal 1.0 then:

$$\frac{\int BTDF_i}{\int BRDF_i} = \frac{T}{R} \tag{5}$$

Where R and T are the Fresnel terms.

Between 0 and 1.0, the amplitude of the isotropic and lambertian component of the BTDF and BRDF will show a partial dependency on the Fresnel terms. The amplitude of Specular lobe components always depend on the Fresnel terms. This simple approach has the flexibility to allow parameters to be easily fitted to represent experimental data. The impact of each parameter is easy to understand and to adjust.

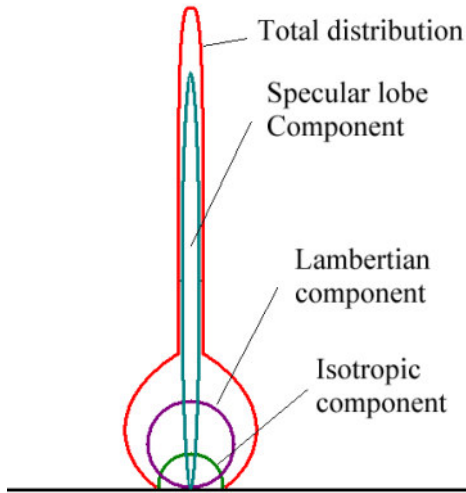


Fig. 7. Rough surface component model BRDF

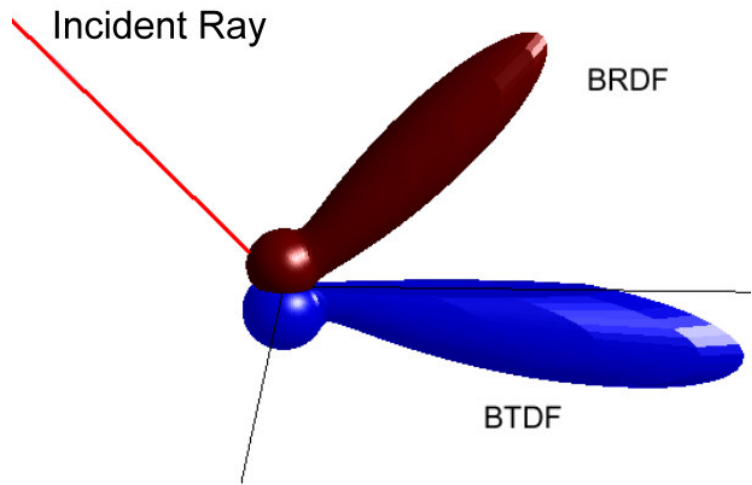
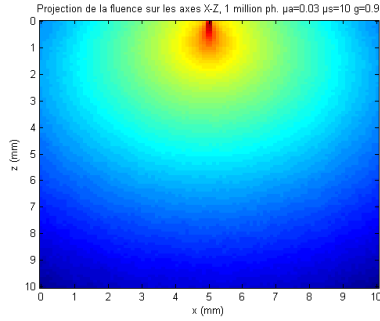
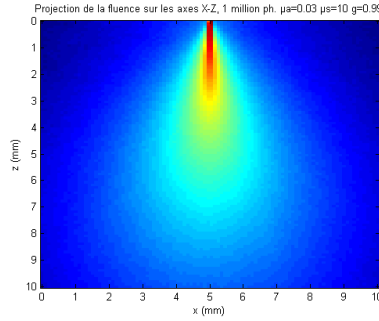


Fig. 8. Example of a BSDF for a specific incident ray angle

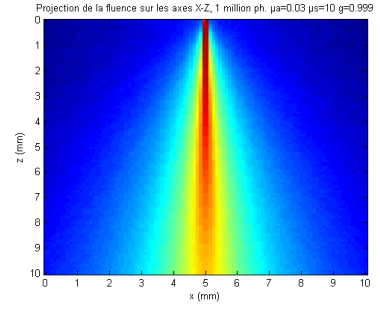
An important advantage of this approach is that it is straightforward to model by Monte Carlo. Using the percentages of isotropic, lambertian and specular lobe components, a simple random variable is used to select randomly which component affects a specific photon packet at a rough surface interface. Components distribution are invertible, so the inverted sampling function is then used to reflect and refract the photons packets, taking also into account the Fresnel dependency and reflection/refraction angles for the specular lobes.



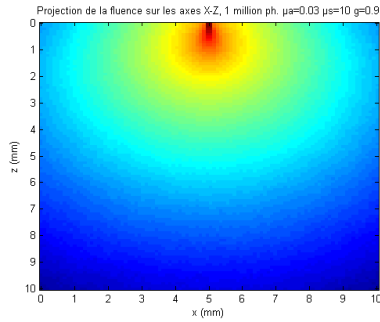
a) Specular surface $g=0.90$



b) Specular surface $g=0.99$

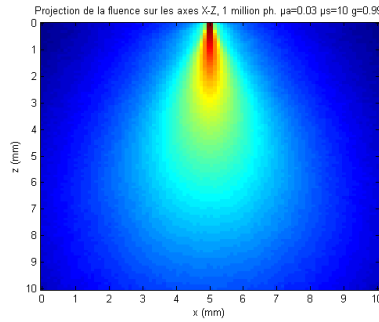


c) Specular surface $g=0.999$



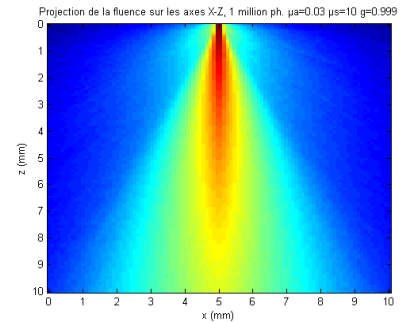
d) Rough surface $g=0.90$

[iso.=2%, lb.= 10%, sp.=88% $\sigma_\theta = 10^\circ$]



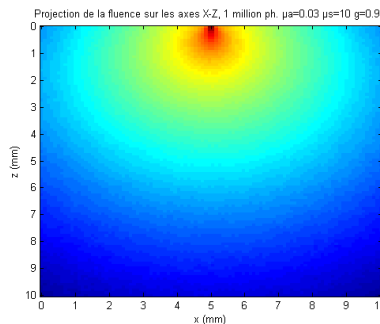
e) Rough surface $g=0.99$

[iso.=2%, lb.= 10%, sp.=88% $\sigma_\theta = 10^\circ$]



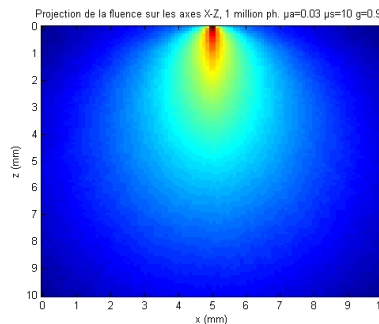
f) Rough surface $g=0.999$

[iso.=2%, lb.= 10%, sp.=88% $\sigma_\theta = 10^\circ$]



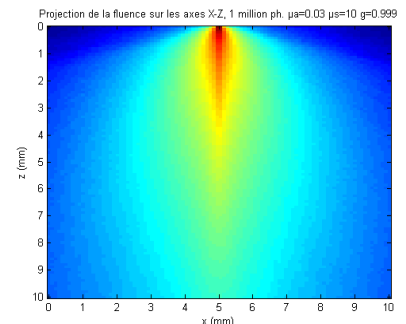
g) Rough surface $g=0.90$

[iso.=5%, lb.= 20%, sp.=75% $\sigma_\theta = 30^\circ$]



e) Rough surface $g=0.99$

[iso.=5%, lb.= 20%, sp.=75% $\sigma_\theta = 30^\circ$]



h) Rough surface $g=0.999$

[iso.=5%, lb.= 20%, sp.=75% $\sigma_\theta = 30^\circ$]

Fig. 9. Effect of surface roughness as a function of anisotropy

Fig.9 illustrates an example of the effect of rough surfaces as a function of anisotropy. We observe that for higher scattering medium (Fig. 9 a, d and g), the effect of the rough surface is localized near the source, while for a low scattering medium (Fig. 9 c, f and h) the impact is more important, even at a farther distance from the source.

3.4 Fluorescence modeling

The strategy used to model fluorescence is the following: for photon packet going through a region containing fluorophores, we take into account the concentration, extinction coefficient and quantum efficiency of the fluorophore and start new fluorescence packets along the primary photon packet path as shown in Fig. 10.

The number of fluorescent packets to start can be variable as a function of the type of simulation and the geometry used. A proposed strategy is to use criteria like a number of new photon packets per millimeter inside the fluorescent region, which is rounded to highest integer value. For example, if a photon path inside a fluorescent region is 7.69 mm, then 8 new fluorescent photon packets can be started. The primary photon packet path inside the fluorescent region is then cut in 8 equal-length sub-paths. For each sub-path, the number of absorbed photons is calculated as follows:

$$N_{\text{photon}}_{\text{AbsTotal}} = I_0 \cdot (10^{-\varepsilon C L_n} e^{-\mu_a L_n} - 10^{-\varepsilon C L_{n+1}} e^{-\mu_a L_{n+1}}) \quad (6)$$

Knowing that an equivalent fluorophore absorption could be calculated from:

$$\mu_{af} = -\ln(10^{-\varepsilon C}) \quad (7)$$

Then, we can calculate the fraction of photons absorbed by the fluorophore relative to the total absorption from:

$$F_{\text{absf}} = \frac{\mu_{af}}{\mu_{af} + \mu_a} \quad (8)$$

Taking into account the quantum efficiency, this allows the calculation of the number of fluorescent photons in the new fluorescent photon packets:

$$N_{\text{photon}}_{\text{Fluo}} = Q_{\text{eff}} \cdot N_{\text{photon}}_{\text{AbsTotal}} \cdot F_{\text{abs}} \quad (9)$$

Then after, the position of the new fluorescent photon packet is randomly defined following the statistical decrease of photon packet intensity caused by the absorption.

$$\Delta L = \frac{-\ln(\text{rand})}{\mu_{af} + \mu_a} \quad (10)$$

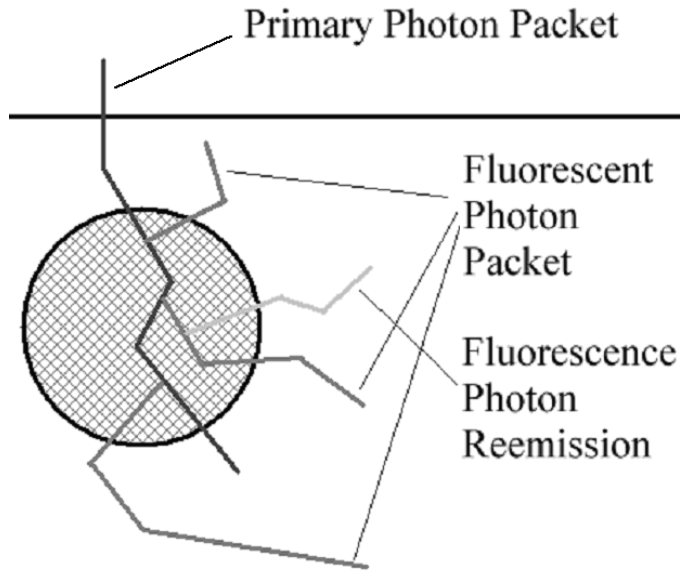


Fig. 10. Fluorescence emission and reemission process

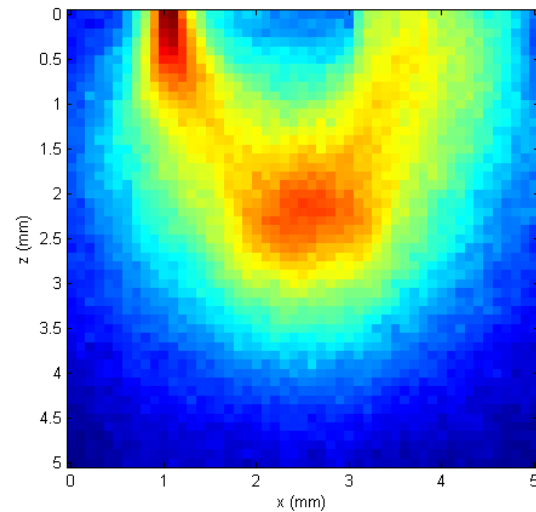


Fig. 11. Sensitivity pattern of fluorescent detected photons for a 2mm diameter fluorescent sphere at 3 mm depth with $C=10\mu\text{M}$, $\epsilon=250000 \text{ M}^{-1}\text{cm}^{-1}$, $Q_{\text{ef}}=0.20$ in a bulk scattering medium of $\mu_s=10 \text{ mm}^{-1}$, $\mu_a = 0.03 \text{ mm}^{-1}$ and $g=0.90$ Source-Detector separation of 3mm, reflection mode acquisition.

To simulate reabsorption and reemission processes, the new fluorescent photon packets, could themselves generate also new packets and the spectral absorption and the emission spectral response of the fluorophores could also be taken into account.

Figure 11 shows the projected fluence of detected fluorescent photon from a simulated fluorescent sphere embedded inside a scattering medium.

4. CONCLUSION AND FUTURE WORK

4.1 Conclusion

In this article, we proposed an approach to eliminate time-distance sampling in the Monte Carlo simulation. We consider that this improvement provides more accurate and higher precision results by reducing the sampling and discretization artifacts. Quantification is also improved by using a full path integration approach in the fluence calculation. We have shown that voxelized geometry is not able to manage reflection and refraction of inclined interfaces adequately. Using meshed objects allows representation of complex heterogeneous medium and to adequately manage reflection and refraction for curved surfaces. In this way, the entire mouse anatomy could be modeled and simulated. We have also proposed a very simple rough surface model to manage reflection and refraction at rough surfaces having refractive index mismatches. We have also presented a simple way to simulate fluorescence processes, allowing us to simulate very complex fluorophore distribution.

There is a processing cost involved in adding those improvements to the MC simulation. This cost should be weighted against the advantages, which depend on the application and the simulation goals. For large volume simulations with fiber optics surface excitation and detection, the gain of the proposed approach could be negligible compare to the processing cost. But for small volumes simulations, or for low scattering medium, or for system configuration with free

beam excitation and detection, we believe that the proposed simulation improvements would provide very important gains in precision, accuracy and results quantification.

4.2 Future work

There are many challenges linked to the current proposed improvements. The first being the computational optimization. For complex heterogeneous medium, reducing the number of surface elements intersection tests is of crucial importance, since for highly scattering medium, those intersection tests forms the main processing burden of the simulation. Therefore, we are looking at ways to further structure the boundary elements hierarchically and spatially to eliminate any unnecessary intersection tests.

Rough surface model parameters need to be fitted using experimental data. It would be interesting to evaluate typical animals BSDF. External BRDF could be obtained with goniometric measurements, but BTDF could be challenging to obtain precisely. It might even be impossible to obtain for internal organs interfaces. Further work should be done to determine the effect of internal rough surface and refractive index mismatches.

Simulation of the effect of reabsorption and reemission phenomenon in function of fluorophore concentration and the impact on measured fluorescence lifetime would be very interesting.

The implemented simulation uses a monochromatic source and it would be very interesting to simulate a wide spectral band source and taking into account the spectral dependency of the optical properties of the medium and also the spectral characteristics of endo/exo fluorescent compounds.

Simulating animal's background endo-fluorescence is of special interest to give valuable data cases for the development of endo/exo fluorescence signal separation algorithms.

Other phenomenon like fluorophore population excitation saturation that causes a nonlinear temporal dependency of the fluorescent emission in function of the source power is not modeled by the current approach and could be interesting.

Finally, complex heterogeneous model opens doors to many interesting simulation allowing us to better understand complex photon diffusion processes and fluorescent phenomenon.

REFERENCES

- ¹ N. Metropolis, THE BEGINNING of the MONTE CARLO METHOD ,Los Alamos Science Special Issue 1987
- ² S. Ulam, R. D. Richtmeyer and J. Von Neumann, "STATISTICAL METHODS IN NEUTRON DIFFUSION" LAMS-551, Los Alamos National Laboratory report (1947)
- ³ N. Metropolis and S. Ulam, THE MONTE CARLO METHOD," J. Am. Statistical Association, vol. 44, pp. 335–341, 1949.
- ⁴ B. C. Wilson and G. Adam, "A Monte Carlo model for the absorption and flux distributions of light in tissue," Med. Phys., vol. 10, pp. 824–830, 1983.
- ⁵ S. A. Prahl, M. Keijzer, S. L. Jacques, A. J. Welch, A MONTE CARLO MODEL OF LIGHT PROPAGATION IN TISSUES,1989 The University of Texas at Austin (USA),Department of Dermatology, Wellman Laboratory,Harvard Medical School (USA)
- ⁶ D. A. Boas, J. P. Culver, J. J. Stott, A. K. Dunn,THREE DIMENSIONAL MONTE CARLO CODE FOR PHOTON MIGRATION THROUGH COMPLEX HETEROGENEOUS MEDIA INCLUDING THE ADULT HUMAN HEAD, NMR Center, Massachusetts General Hospital, Harvard Medical School, Charlestown, MA 02129 Optical Society of America 2002
- ⁷ S. L. Jacques, "Light distributions from point, line and plane sources for photochemical reactions and fluorescence in turbid biological tissues," Photochem Photobiol 67(1), 23-62 (1998).
- ⁸ Lihong Wang Steve L. Jacques MCML- MONTE CARLO MODELING OF LIGHT TRANSPORT IN MULTILAYERED TISSUES, Computer Methods and Programs in Biomedicine 47 (1995) 131-146
- ⁹ Xiaoyan Ma, Jun Qing Lu, and Xin-Hua Hu, Effect of surface roughness on determination of bulk tissue optical parameters, OPTICS LETTERS, Vol. 28, No. 22 , November 15, 2003

- ¹⁰ Guobin Ma, Jean-François Delorme, Pascal Gallant, David A. Boas, Comparison of simplified Monte Carlo simulation and diffusion approximation for the fluorescence signal from phantoms with typical mouse tissue optical properties, *Applied Optics*, Vol. 46, Issue 10, pp. 1686-1692 (2007)
- ¹¹ IUPAC Compendium of Chemical Terminology 2nd Edition (1997)
- ¹² ICRU 33: Radiation Quantities and Units, April, 1980
- ¹³ Tomas Möller and Ben Trumbore, "Fast, Minimum Storage Ray-Triangle Intersection", "journal of graphics tools", volume 2, number 1, pages 21-28, 1997
- ¹⁴ Didier Badouel, An Efficient Ray-Polygon Intersection, in *Graphics Gems*, edited by Andrew S. Glassner, Academic Press inc., 1990, pp. 390-393.
- ¹⁵ W.P. Segars, B.M.W. Tsui, E.C. Frey, G.A. Johnson, and S.S. Berr, "Development of a 4D digital mouse phantom for molecular imaging research", *Molecular Imaging & Biology*, Vol. 6, Issue 3, p. 149-159, 2004.
- ¹⁶ Yinlong Sun, Statistical ray method for deriving reflection models of rough surfaces, *J. Opt. Soc. Am. A*/Vol. 24, No. 3/March 2007
- ¹⁷ Bruce Walter, Stephen R. Marschner, Hongsong Li, Kenneth E. Torrance, *Microfacet Models for Refraction through Rough Surfaces*, Eurographics Symposium on Rendering, 2007